Clinical, Cosmetic and Investigational Dermatology

Dovepress
Taylor & Francis Group

Open Access Full Text Article

ORIGINAL RESEARCH

Exploration of Targets Potentially Linked to IL-17A Inhibitor Response in Psoriasis Using Machine Learning

Yan Wei*, Meng Liu*, Kuan-Hou Mou, Li-Juan Wang, Yan Zheng

Department of Dermatology, The First Affiliated Hospital of Xi'an Jiaotong University, Xi'an, Shaanxi, 710061, People's Republic of China

*These authors contributed equally to this work

Correspondence: Yan Zheng; Li-Juan Wang, Email zenyan66@126.com; 6945216juan@163.com

Background: This study aimed to elucidate IL-17 inhibitors' mechanisms in psoriasis, offering a theoretical basis for tackling clinical issues like treatment resistance and relapse.

Methods: Datasets GSE226244 and GSE31652 served as the training set, and GSE201827 served as the testing set. Differential hub genes post-IL-17 inhibitor treatment identified via Limma and WGCNA. DEGs were defined by a |log2 fold-change (FC)| greater than 0.585 and a stringent FDR threshold of less than 0.05. CIBERSORT evaluated immune cell infiltration. Comprehensive analysis of 113 machine learning methods identified optimal predictive model. qPCR validated CLCNKB and GFRA3 expression in psoriasis cell models post-IL-17 inhibitor treatment. Mendelian randomization analysis explored causal links between CLCNKB, GFRA3 and cytokines.

Results: Analysis of gene expression in psoriasis patients treated with IL-17 inhibitors identified 95 differential genes enriched in FoxO signaling, Lysine degradation, and cGMP-PKG pathways. The LASSO-glmBoost (a hybrid machine learning method combining Lasso regularization with gradient boosting) model exhibited superior diagnostic performance (AUC: 0.920 in training, 0.858 in test), highlighting CLCNKB and GFRA3 as key genes in the optimal predictive framework. qPCR confirmed their upregulation in IL-17-inhibitor-treated psoriasis cells, and Mendelian randomization linked both genes causally to cytokine dysregulation.

Conclusion: The study reveals new insights into IL-17 inhibitors' mechanisms in psoriasis, suggesting that upregulation of CLCNKB and GFRA3, along with cytokine dysregulation (eg, IL-13, IL-10, IL-12, TGF-β, TNF-α), may underlie potential resistance and relapse in patients. This work demonstrates a novel approach to clinical outcome prediction with potential utility for specific clinical application, warranting further validation in clinical settings.

Keywords: psoriasis, IL-17A inhibitors, machine learning, mendelian randomization, immune cell infiltration

Introduction

Psoriasis (Ps) is a chronic inflammatory disorder with multi-system involvement, characterized by cutaneous manifestations and significant associations with metabolic syndrome, psoriatic arthritis, and cardiovascular comorbidities[1,2] The pathogenesis of Ps is complex, intricately involving immune, genetic, and environmental factors.[3–5] Early research in the 1980s identified CD4+ T-helper cell subsets as key drivers, and subsequent studies have demonstrated that Th1 cells (secreting IFN-γ) and Th17 cells (secreting IL-17/IL-22) play dominant roles in coordinating keratinocyte hyperproliferation, dendritic cell activation, and neutrophil recruitment.[6–11] Based on this understanding of psoriasis pathogenesis, biologics specifically targeting core inflammatory cytokines, such as IL-17 and TNF-α, have been widely adopted in clinical practice, offering significant benefits to psoriasis patients.[12,13] While highly effective, the use of biologics in psoriasis treatment is not without risks. For instance, anti-IL-17 monoclonal antibodies may lead to disease progression during treatment by enabling psoriasis to bypass the blockade pathway. Alternatively, they may shift the inflammatory profile from a predominantly Th1-driven response to a Th2-driven response, resulting in eczema-like manifestations.[14,15] A major clinical challenge is the development of treatment resistance. Some patients show no clinical or molecular

Received: 10 September 2025
Accepted: 12 December 2025
Published: 25 December 2025

response to biologics upon initial treatment, termed primary non-response. Others may experience secondary loss of response, where initially effective treatment gradually becomes ineffective due to acquired resistance.[16,17] The transcriptomic contrasts before and after IL-17A inhibitor treatment may reveal: In primary non-response, baseline expression defects or inhibitory epigenetic marks in key genes of the IL-17A signaling pathway; In secondary loss of response, persistent activation of IL-17A inhibitor-induced negative feedback pathways or aberrant upregulation of genes associated with effector cell exhaustion.

Therefore, conducting in-depth research on the mechanism of action of IL-17 inhibitors in psoriasis holds significant research value and clinical importance. This study employed multiple machine learning diagnostic model analyses on transcriptome sequencing data obtained from skin lesions of psoriasis patients before and after treatment with IL-17A inhibitors. The primary objective was to investigate gene expression changes, immune cell infiltration characteristics, and pathway enrichment following the blockade of the IL-17-mediated pathway. This study aims to provide potential solutions and a theoretical foundation for addressing critical clinical challenges such as treatment non-responsiveness, drug resistance, and recurrence encountered in the current clinical use of IL-17 inhibitors.

Materials and Methods

Data Acquisition and Preprocessing

The specific workflow of this study is illustrated in Figure 1. This study utilized microarray data from the Gene Expression Omnibus (GEO, http://www.ncbi.nlm.nih.gov/geo), a public repository of gene expression datasets. This study was exempt from ethical review, per Article 32(1) and (2) of China's Ethical Review Measures for Life Science and Medical Research Involving Human Subjects (promulgated on February 18, 2023). Specifically, the GSE226244 (n=33 psoriasis pre-treatment, n=28 psoriasis post-treatment, n=8 normal controls), GSE31652 (n=24 psoriasis pre-treatment,

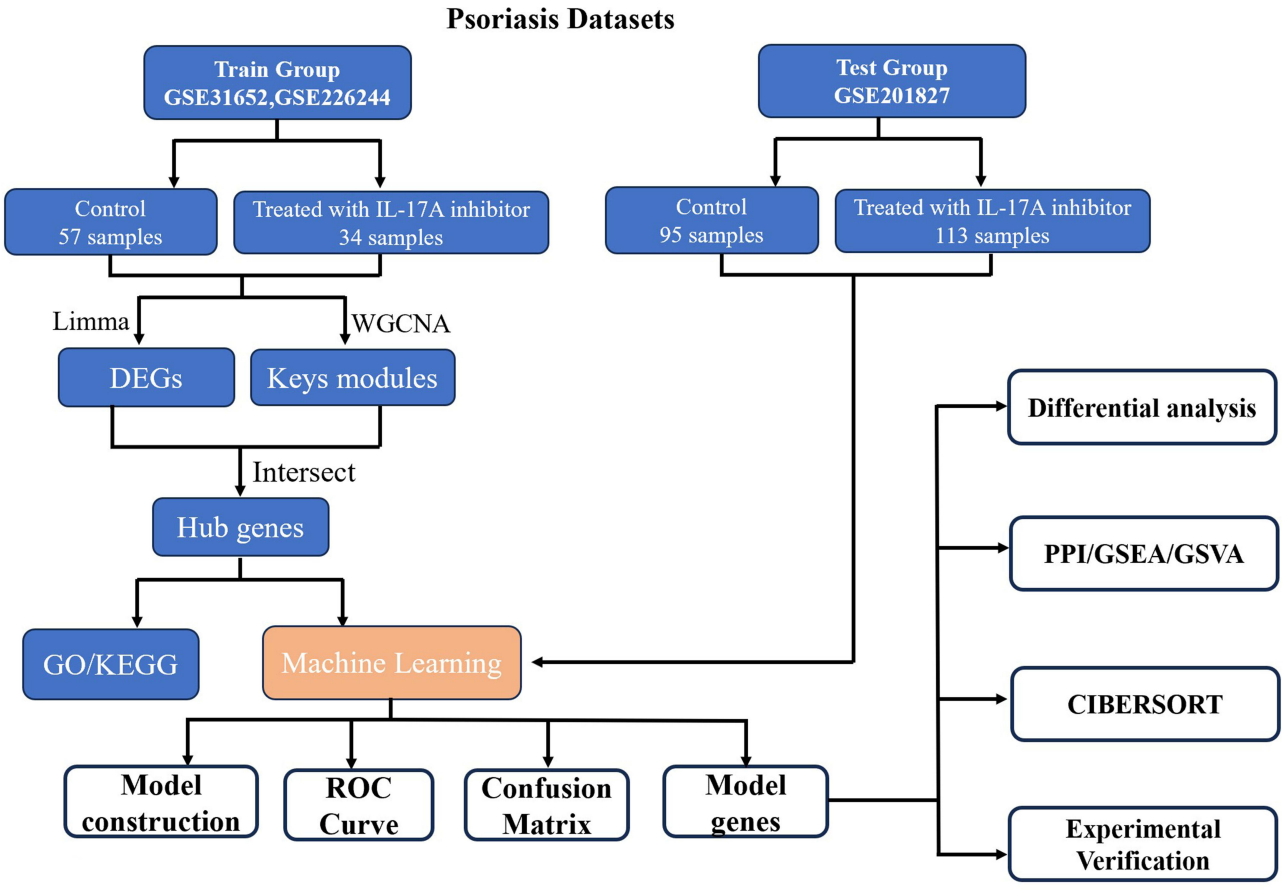

Figure 1 Flowchart Illustrating the Research Methodology.

n=6 psoriasis post-treatment), and GSE201827 (n=95 psoriasis pre-treatment, n=113 psoriasis post-treatment) datasets were obtained from GEO, encompassing total RNA extracted from epithelial cells of psoriasis patients before and after IL-17A inhibitor treatment. The time points in the training set primarily correspond to 12 weeks post-treatment, while those in the validation set mainly focus on 52 weeks post-treatment. Datasets GSE226244 and GSE31652 served as the training set (n=91), and GSE201827 served as the testing set (n=208). Using a *t*-test to compare model performance, with an effect size (d) set at 0.5, a post hoc power analysis was conducted in GPower to confirm the adequacy of the sample size. Detailed information on these datasets is provided in Table 1. To ensure data consistency for analysis, the datasets were preprocessed using the SVA package (version 4.2.1) in R software. This preprocessing included gene ID conversion, clinical information extraction, batch effect correction and integration, and homogenizationon the psoriasis datasets GSE226244 and GSE31652. Homogenization transformed data from different batches into a common basis, followed by principal component analysis (PCA) to confirm the effectiveness of batch effect removal.

Identification of Differentially Expressed Genes (DEGs)

This study utilized the Limma package in R to identify DEGs between 57 control cases and 34 treatment cases with IL-17A inhibitors. Limma, a type of generalized linear model, enables the identification of DEGs between different experimental groups. To control for multiple comparisons, the false discovery rate (FDR) was employed to adjust *p*-values. DEGs were defined by a |log2 fold-change (FC)| greater than 0.585 and a stringent FDR threshold of less than 0.05.

Weighted Gene Co-Expression Network Analysis (WGCNA)

WGCNA, a systematic biological approach, constructs gene co-expression networks to identify modules of genes associated with specific traits. This method investigates co-expression patterns and functional relationships among genes by analyzing gene expression data. It identifies genes with similar expression patterns and clusters them into distinct modules based on their co-expression profiles.[18] Genes within these modules often share similar biological functions. The process involves several steps: 1) data quality assessment and preprocessing, including handling missing values, clustering samples, data matching, and transforming the expression matrix into a correlation matrix; 2) selection of an appropriate soft threshold (β) using the pickSoftThreshold function to ensure scale-free network properties in the adjacency matrix (In this study, β=8); 3) conversion of the adjacency matrix into a topological overlap matrix (TOM) based on the Topological Overlap Measure, which reflects the degree of association between genes; 4) hierarchical clustering of genes based on the TOM-based dissimilarity measure (1-TOM) to group genes with similar expression patterns into modules; and 5) identification of gene co-expression modules using dynamic tree-cutting algorithms. Finally, the method calculates the correlation between module eigengenes, modules, and phenotypes, selects the module with the highest correlation, and computes module identity and gene significance to extract key genes within the selected module.

Functional Enrichment Analysis

This study employed Gene Ontology (GO) and Kyoto Encyclopedia of Genes and Genomes (KEGG) enrichment analyses to elucidate the biological functions, associated signaling pathways, and gene-gene interactions of co-expressed genes. GO encompasses three domains: Biological Process (BP), Molecular Function (MF), and Cellular

Table 1 Basic Information on the Datasets Used in This Study

Datasets	Type	Sample Size		Platform
		Psoriasis	Psoriasis with IL17 Inhibitor	
GSE226244	RNA	33	28	GPL570
GSE31652	RNA	24	6	GPL570
GSE201827	RNA	95	113	GPL570

Component (CC), providing a comprehensive understanding of gene function. KEGG pathway enrichment analysis was performed to identify the cellular pathways potentially dysregulated in the context of differential gene expression.

Machine Learning

Machine learning encompasses a suite of algorithms and research methodologies that enable machines to learn from data. This involves analyzing vast datasets to identify patterns and subsequently utilize these patterns to make predictions.[19] The study employs a supervised learning approach for analysis. In this study, 113 distinct machine learning methods were implemented to screen core model genes in both the control and treatment groups of patients. The specific algorithms used in this study are detailed in Supplementary Material 1. In machine learning, feature engineering is a critical step to enhance model performance, with its core processes primarily including data preprocessing, feature construction, feature selection, feature transformation, and feature dimensionality reduction using PCA. To ensure data integrity, we implemented stringent measures to prevent data leakage. All preprocessing steps (such as scaling and imputation) were performed independently on the training and test sets. Where applicable, temporal or spatial partitioning was applied, with explicit validation of independence. For model evaluation, we utilized a nested CV framework (5-fold outer CV, 3-fold inner CV) for model training and evaluation. To mitigate class imbalance, we employ SMOTE (Synthetic Minority Oversampling Technique) for synthetic sample generation and Tomek Links to eliminate borderline cases. Hyperparameter optimization was conducted via grid search. All code and scripts used in this study are publicly available in Supplementary Material 2. Subsequently, machine learning models were constructed based on these analyses. Through rigorous evaluation and validation of the performance of each model, the optimal and robust machine learning model for this study was selected.

Analysis of Signaling Pathways Related to Hub Genes

To investigate the interaction networks and signaling pathways involving the six identified genes, we employed the GENEMANIA database (http://genemania.org/). Next, we utilized gene set enrichment analysis (GSEA) to explore gene enrichment patterns across different risk groups. Following this, we performed an analysis of GO term and KEGG pathway enrichment. Gene Set Variation Analysis (GSVA), in contrast to GSEA, is a non-parametric and unsupervised method. Unlike GSEA, which requires samples to be pre-grouped, GSVA calculates enrichment scores for specific gene sets within each sample. This enables the comparison of gene set expression patterns across different treatment groups, revealing enriched signaling pathways.

Immune Infiltration Analysis

The CIBERSORT algorithm, a deconvolution method, infers the relative abundance of 22 distinct human immune cell types within a mixed sample based on gene expression profiles. This is achieved by deconvolving the observed gene expression data with a reference matrix containing gene expression signatures of known immune cell types.[20,21] The algorithm estimates the cellular composition by minimizing the difference between the observed and predicted gene expression profiles, effectively determining the proportion of each immune cell type contributing to the overall gene expression signal. The results are typically visualized using bar charts to depict the proportion of each immune cell type in each sample. Furthermore, the "corrplot" R package can be utilized to generate a heatmap illustrating the correlations among the 22 identified immune cell types. Finally, violin plots were generated to visualize and compare the distributions of immune cell proportions between the control and treatment groups.

Mendelian Randomization Study

In this study, the exposure data were sourced from the GWAS website (https://gwas.mrcieu.ac.uk/datasets/), and the outcome data were obtained from the FinnGen database (https://www.finngen.fi/en/access_results). For the selection of instrumental variables, we utilized cis-eQTLs (tissue-specific $P < 5\times10^{-8}$) and applied strict linkage disequilibrium removal (r^2=0.001, kb = 10,000). The harmonize data function was employed to align effect alleles, and palindromic variants were excluded. All instrumental variables had F-statistics > 10 to mitigate weak instrument bias. Additionally, Bonferroni correction was applied for multiple testing, and MR-PRESSO was employed to identify and correct for outliers. A Mendelian randomization analysis

(http://app.mrbase.org/) investigating the causal relationship between *GFRA3, CLCNKB*, and cytokine levels was performed, utilizing the widely accepted Inverse Variance Weighting (IVW) method for its reliability in calculating the weighted average effect size across all instrumental variables.[22] Following this analysis, horizontal pleiotropy and heterogeneity tests were implemented to ensure the validity of the results.[23,24]

Cell Culture and Establishment of the Psoriatic Cell Model

The HaCaT cells purchased from ATCC were cultured in DMEM containing 10% fetal bovine serum, penicillin (100 U/mL), and streptomycin (100 μg/mL) at 37 °C in a humidified atmosphere with 5% carbon dioxide. Subsequently, the HaCaT cells were stimulated with M5 (TNF-α, IL-17A, IL-22, IL-1α, and oncostatin M) at a concentration of 10 ng/mL for 24 hours, as previously described.[25] For IL-17 inhibition, the HaCaT cells were first treated with M5 for 24 hours, followed by treatment with Secukinumab (MCE, USA, cat. No. HY-P9927, 10 ng/mL) for 1 hour.

qRT-PCR

Total RNA was extracted from HaCaT cells using an RNA Isolation Kit (Aidlab Biotechnologies, China) and subsequently reverse transcribed into cDNA using a reverse transcription kit (Aidlab Biotechnologies, China). q-PCR was performed on the BioRad CFX96 system. Each reaction was carried out in triplicate. β-actin was used as an internal reference for analysis. The primer sequences used in this study are as follows:

CLCNKB: F 5'- GTGGGCATAGTGCGAAGGG-3',
CLCNKB: R 5'- CAAAGAGGTTGTGTGCCTCAT-3',
GFRA3: F 5'- TGCACCTCTAGCATAAGCACC-3',
GFRA3: R 5'- TGCAGCCTATCAGAGAGCTGT-3',
β-actin: F 5'-GAAGATCAAGATCATTGCTCCT-3',
β-actin: R 5'- TACTCCTGCTTGCTGATCCA-3'.

Statistical Analysis

All data were processed and analyzed using R software (https://www.r-project.org/) and Perl (Practical Extraction and Report Language). Differences between variables were assessed using the Student's *t*-test and the chi-square test. For data that did not follow a normal distribution, non-parametric tests were employed. For gene-level analysis, independent t-tests were performed to compare expression levels between groups, after confirming normality via Shapiro–Wilk tests. For immune-cell proportion analysis, chi-square (χ^2) tests were used to assess differences in proportions, as the data were categorical. For qPCR data, non-parametric tests (Mann–Whitney U) were applied for comparisons where normality assumptions were violated. A significance level of $p < 0.05$ was used throughout the analysis.

Results

Data Preprocessing and Identification of DEGs

In this study, datasets GSE226244 and GSE31652 served as the training set, and GSE201827 served as the testing set. Using the SVA package (version 4.2.1) in R, we performed gene ID conversion, clinical information extraction, batch effect correction and integration, and homogenization of the psoriasis datasets GSE226244 and GSE31652. The resulting training dataset comprised 57 control samples and 34 samples from patients treated with an IL-17A inhibitor. Evaluation of the data confirmed the effectiveness and reliability of the preprocessing. Box plots demonstrated significant differences in sample distributions across datasets before batch effect removal, indicating the presence of batch effects. Following batch effect correction, the sample distributions became consistent across datasets (Figure 2A and B). PCA confirmed consistency in the principal components after processing, demonstrating the suitability of the data for further analysis (Figure 2C and D). Using the Limma package in R, DEGs were identified. A total of 2200 DEGs were identified between the two patient groups, comprising 1126 upregulated and 1074 downregulated genes. Heatmaps and volcano plots were generated to visualize these DEGs (Figure 2E and F).

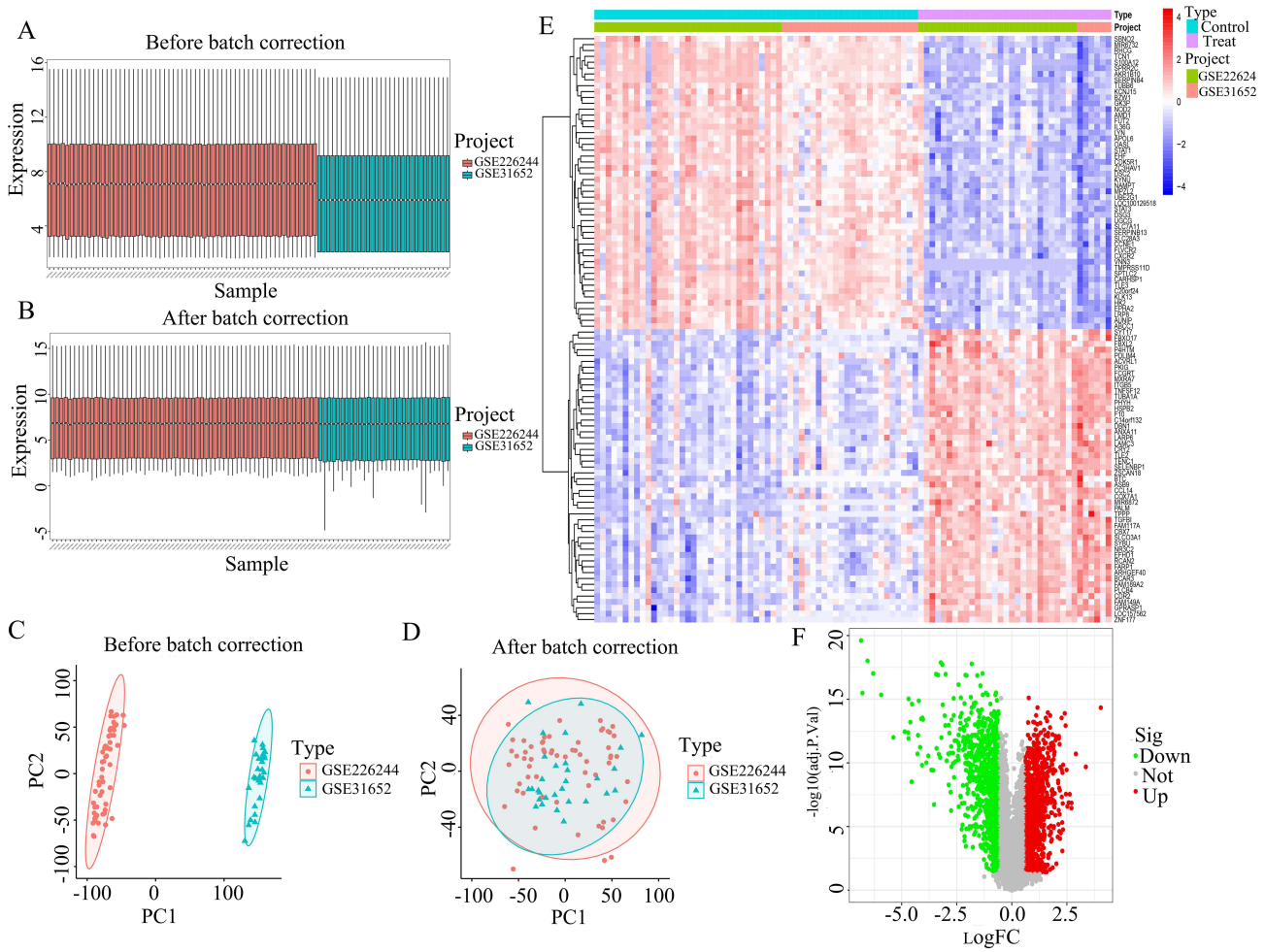

Figure 2 Data preprocessing and Identification of DEGs (**A**) Boxplot before batch correction. (**B**) Boxplot after batch correction. (**C**) Principal component analysis of the two original Psoriasis datasets before batch effect correction. (**D**) Principal component analysis of the corrected Psoriasis dataset. (**E**) Heatmap of DEGs between the control group and treatment group. (**F**) Volcano plot of DEGs between the control group and treatment group.

Construction of Weighted Gene Co-Expression Networks and Identification of Modules

WGCNA was performed on the training dataset. Figure 3A demonstrates that, with a power value of 8, the scale-free fit index reached 0.883 with relatively low average connectivity, consistent with the characteristics of a scale-free network. Following WGCNA, nine distinct characteristic modules were identified (Figure 3B). Among these modules, the module eigengenes in the pink module exhibited the highest correlation (r=0.91, *p*=4e-35) between the control and treatment groups, with statistical significance (Figure 3C). The importance of feature genes in the nine modules was evaluated. The feature genes in the pink module exhibited the highest importance scores and demonstrated a strong correlation with the module traits (Figure 3D and E).

Functional Enrichment Analysis of Co-Expressed Genes

Figure 2F shows 2200 DEGs between the psoriasis control and treatment groups. WGCNA identified 217 hub genes within the pink module. The intersection of these two gene lists revealed 95 commonly expressed genes (Figure 4A). GO and KEGG pathway analyses were performed on these 95 genes, and the results are presented in Figure 4. GO analysis indicated enrichment of these genes in biological processes, including epithelial tube morphogenesis, embryonic organ development, gonad development, development of primary sexual characteristics, negative regulation of neurogenesis, negative regulation of axonogenesis, and the activin receptor signaling pathway. Cellular component analysis showed

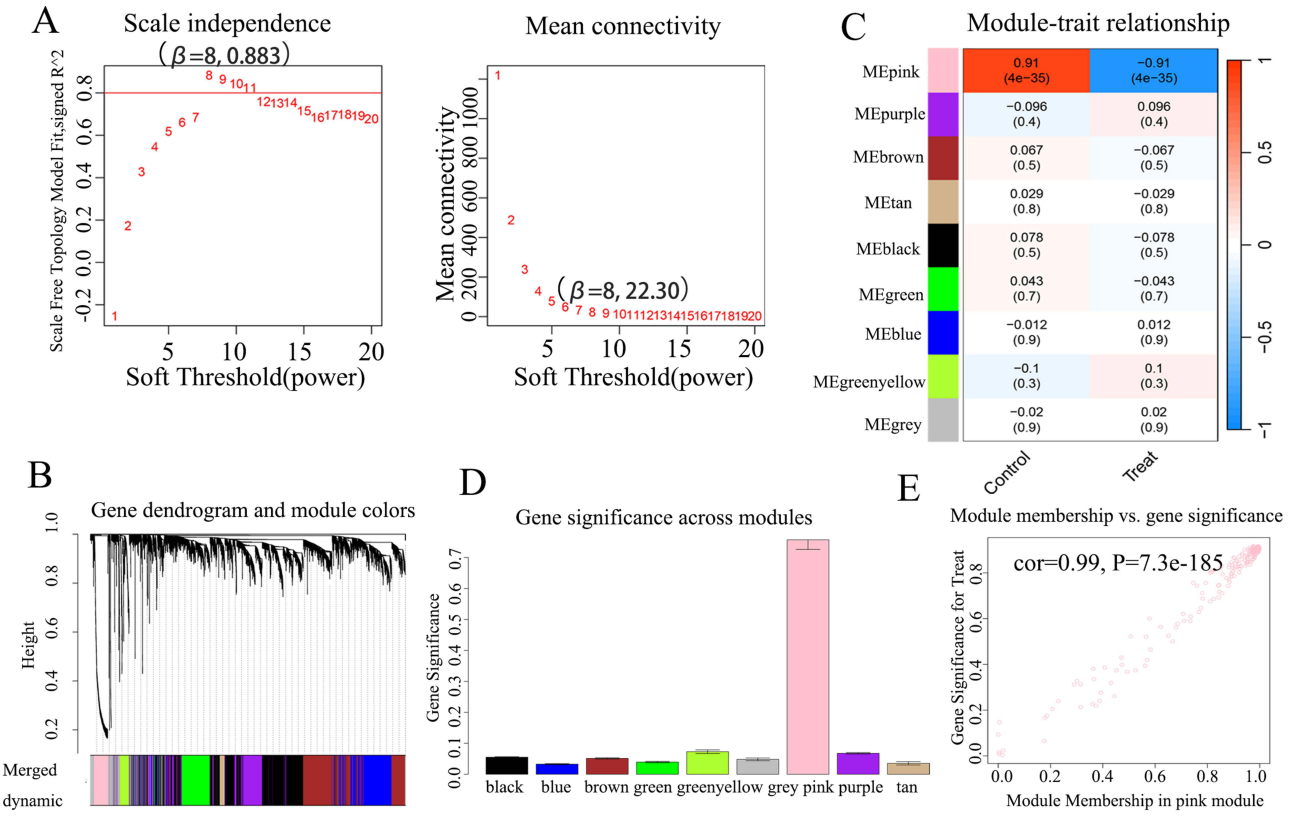

Figure 3 Construction of Weighted Gene Co-expression Networks and Identification of Modules (**A**) Scale Independence and Mean connectivity plots of psoriasis. (**B**) Gene dendrogram distribution in different color modules. (**C**) Traits of different color modules in psoriasis control group and treatment group. (**D**) Importance scoring diagram of feature genes in different color modules. (**E**) The correlation and importance distribution map of characteristic genes in the pink module. Correlation plot between module genes (MM, X-axis) in the pink module and genes in traits (GS, Y-axis).

enrichment in the glutamatergic synapse, synaptic membrane, postsynaptic specialization membrane, an integral component of the postsynaptic membrane, an intrinsic component of the postsynaptic membrane, bicellular tight junction, tight junction, presynaptic membrane, and apical junction complex. Molecular function analysis revealed enrichment in DNA-binding transcription repressor or activator activity, RNA polymerase II-specific basal transcription machinery binding, basal RNA polymerase II transcription machinery binding, UDP-glycosyltransferase activity, and hexosyltransferase activity (Figure 4B-D). KEGG pathway analysis revealed significant enrichment of the co-expressed genes in several signaling pathways, including circadian rhythm, FoxO signaling, Apelin signaling, long-term depression, Cushing syndrome, lysine degradation, the cGMP-PKG signaling pathway, and renin secretion (Figure 4E and F).

Construction and Validation of Machine Learning Models

This study employed 113 distinct machine-learning methods to screen core genes from psoriasis patients in both control and treatment groups and to construct predictive models. Through evaluation and validation of model performance, the optimal model was identified. Figure 5A demonstrates that the model constructed using the Least Absolute Shrinkage and Selection Operator (LASSO)-combined glmBoost algorithm exhibited the highest diagnostic performance. Receiver operating characteristic (ROC) curve analysis revealed that this model achieved an area under the curve (AUC) of 0.920 (95% CI: 0.862, 0.968) in the training set and 0.858 (95% CI: 0.798, 0.911) in the test set, indicating a strong diagnostic value (Figure 5B and C). Performance metrics for the LASSO-combined glmBoost model were as follows: in the training set, accuracy was 92.22%, precision was 88.89%, recall was 98.25%, and the F1 score was 0.9514; in the validation set, accuracy was 83.65%, precision was 76.99%, recall was 91.58%, and the F1 score was 0.8366 (Figure 5D and E). This model identified six differentially expressed genes. Compared to the control group, *CLCNKB, GFRA3, ZNF471, CNKSR2*, and *SSTR1* were significantly upregulated in the treatment group, while *GJA3* was downregulated (Figure 5F and G). Gene

https://doi.org/10.2147/CCID.S557553

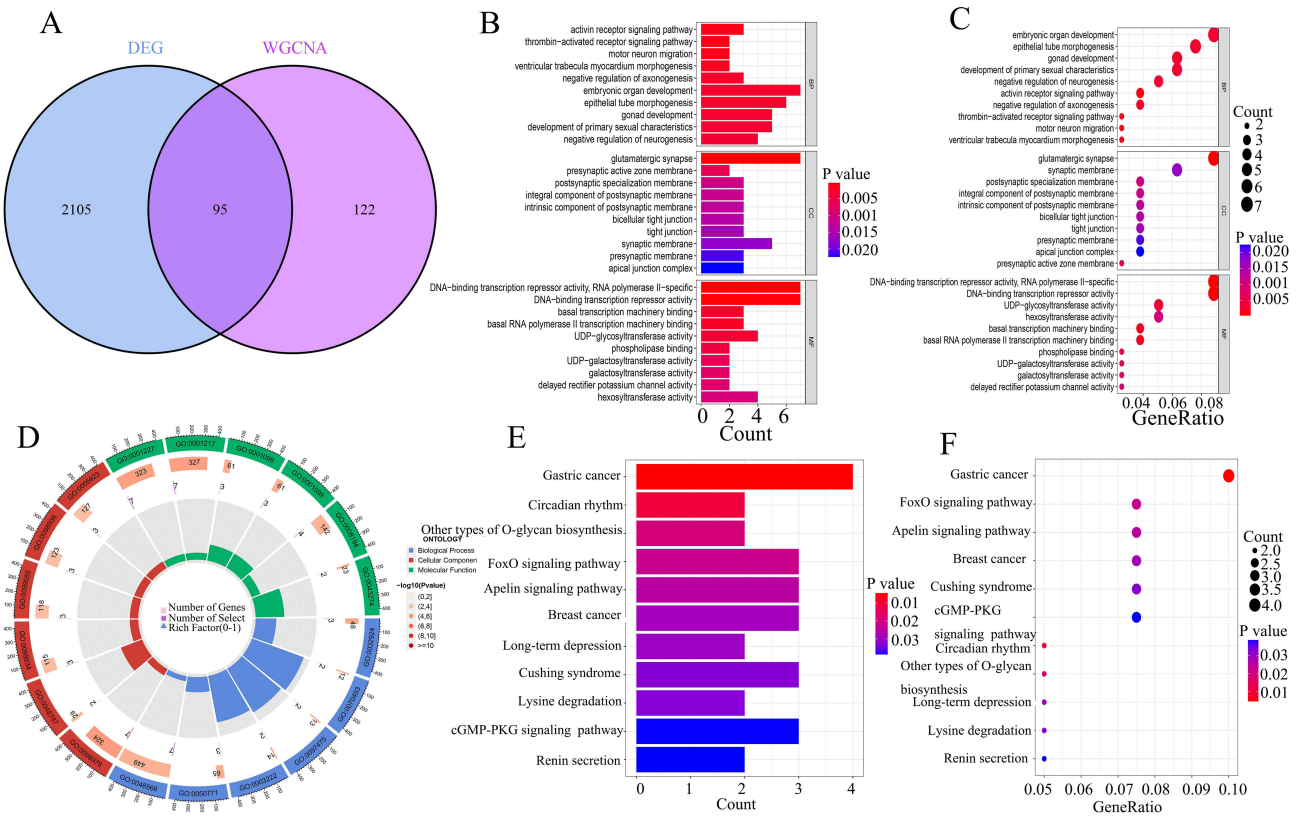

Figure 4 Functional enrichment analysis of co-expressed genes (**A**) Venn diagram of DEGs and module eigengenes of the pink module from WGCNA analysis. (**B**) The barplot chart in GO analysis, where BP stands for Biological Process, CC stands for Cellular Component, and MF stands for Molecular Function. (**C**) Bubble Chart in GO Analysis. (**D**) Circular Graph in GO Analysis. (**E**) The barplot chart for KEGG analysis. (**F**) The bubble chart for KEGG analysis.

correlation analysis revealed significant correlations among these hub genes (Figure 5H). ROC curve analysis for each of these six differentially expressed genes demonstrated high AUC values for *CLCNKB, GFRA3, SSTR1, ZNF471*, and *CNKSR2*, indicating their high accuracy in distinguishing between patients in the psoriasis control and treatment groups (Figure 5I). This suggests a potential involvement of these genes in IL-17-related signaling pathways.

Functional Validation of CLCNKB and GFRA3 via Enrichment Analysis and Cellular Assays

Figure 5 demonstrates that the expression of *CLCNKB* and *GFRA3* is significantly upregulated in psoriasis patients following treatment with an IL-17 inhibitor, correlating with higher AUC values. Consequently, relevant signaling pathways associated with *CLCNKB* and *GFRA3* were further investigated. Using the GeneMania database, the functions of *CLCNKB* and *GFRA3* were predicted, and a gene interaction network was constructed, revealing interactions with multiple proteins that contribute to cellular functions (Figure 6A). GSVA indicated that *CLCNKB* was primarily involved in pathways such as chemokine signaling, natural killer cell-mediated cytotoxicity, antigen processing and presentation, leukocyte transendothelial migration, cytokine-cytokine receptor interaction, base excision repair, and homologous recombination. *GFRA3* was primarily associated with pathways such as T cell receptor signaling and the tricarboxylic acid (TCA) cycle (Figure 6B and C). GSEA suggested that *CLCNKB* and *GFRA3* could participate in processes such as maintaining taste receptor activity (Figure 6D and E). Cellular experiments were conducted to assess the expression levels of *CLCNKB* and *GFRA3* following treatment with M5 alone and in combination with the IL-17 inhibitor HYP9927. Consistent with previous findings, the expression levels of *CLCNKB* and *GFRA3* were upregulated after treatment with the combined M5 and HYP9927 regimen (Figure 6F and G).

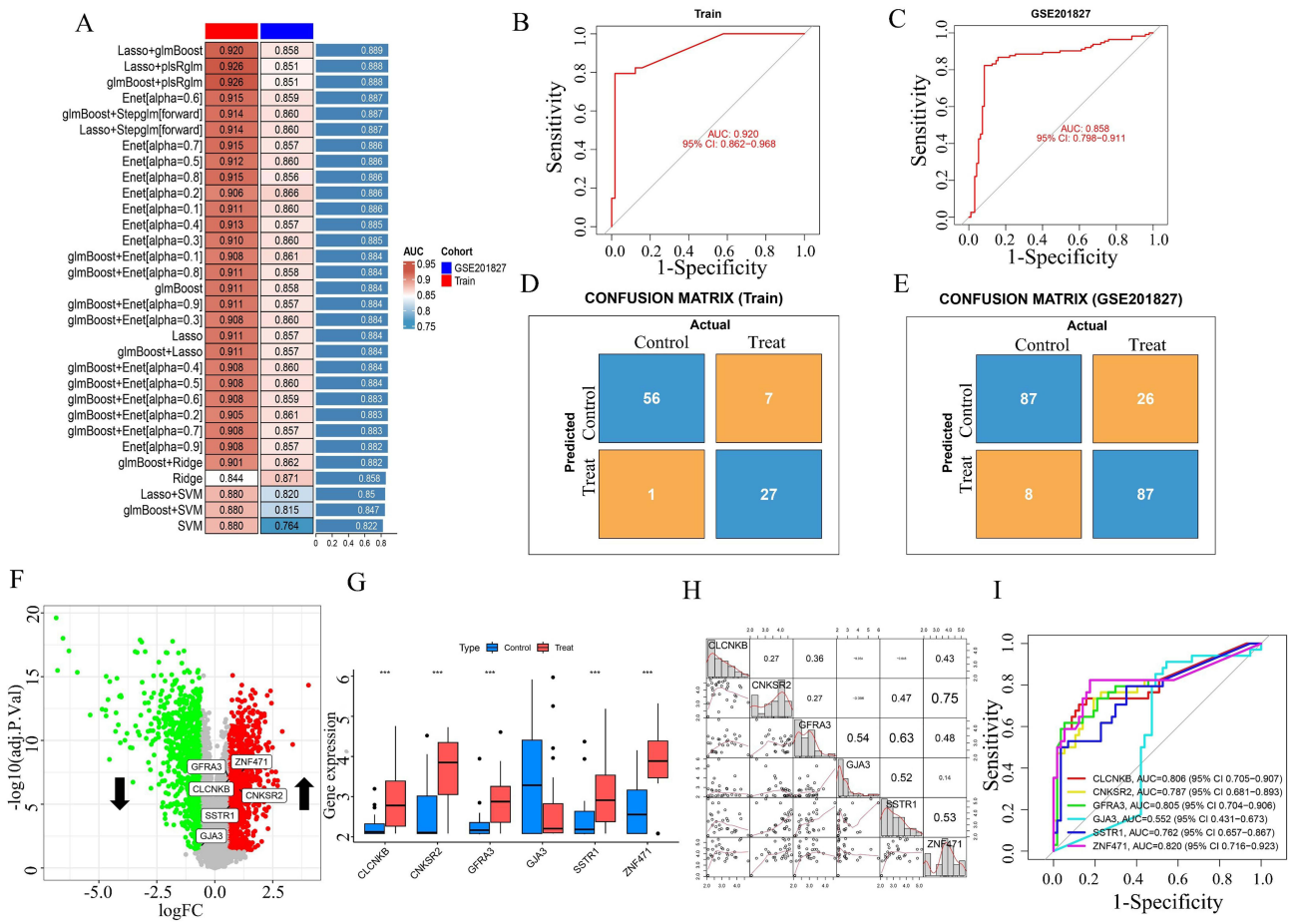

Figure 5 Construction and Validation of Machine Learning Models (**A**) Exhibition of multiple machine learning diagnostic models. (**B**) ROC curve of the training group under the optimal machine learning model. (**C**) ROC curve of the test group under the optimal machine learning model. (**D**) Confusion matrix of the training group. (**E**) Confusion matrix of the test group. (**F**) Volcano plot of the differential model genes. (**G**) Expression levels of differential model genes in the psoriasis control group and treatment group. (**H**) Correlation analysis of differential model genes. (**I**) ROC curve of differential model genes. ***$p<0.001$.

The Immune Cell Infiltration Landscape of Psoriasis Treatment with IL17 Inhibitors

CIBERSORT, a commonly used algorithm for analyzing the distribution of immune cell types in lesional tissues, was employed to analyze immune cell infiltration characteristics in psoriasis patients in both control and treatment groups. Compared with the control group, psoriatic skin lesions treated with IL-17A inhibitors exhibited higher levels of resting mast cells, M2 macrophages, CD8 T cells, and plasma cells, and lower levels of activated dendritic cells, resting dendritic cells, follicular helper T cells, activated CD4 memory T cells, and naïve B cells (Figure 7A and B). Correlation analysis of 22 immune cell types revealed several significant correlations: follicular helper T cells were negatively correlated with regulatory T cells (Tregs) (r = −0.65); resting dendritic cells were negatively correlated with M2 macrophages (r = −0.51); activated dendritic cells were negatively correlated with resting mast cells (r=−0.73); CD8 T cells were positively correlated with Tregs (r = 0.53); memory B cells were positively correlated with naïve CD4 T cells (r=0.68), and naïve CD4 T cells were positively correlated with Tregs (r=0.77) (Figure 7C). After adjusting the CIBERSORT p-value to 0.01, the proportions of key cell types showed no significant changes, demonstrating that the core conclusions are not affected by the threshold selection. The relevant graphics can be found in Figure S1.

Further correlation analysis between the CIBERSORT results and the expression data of the hub genes revealed associations between the expression levels of *CLCNKB, CNKSR2, GFRA3*, and *GJA3* and immune cell infiltration patterns (Figure 7D). Specifically, *CLCNKB* expression was negatively correlated with gamma delta T cell infiltration; *CNKSR2* expression was positively correlated with neutrophil infiltration; *GFRA3* expression was negatively correlated

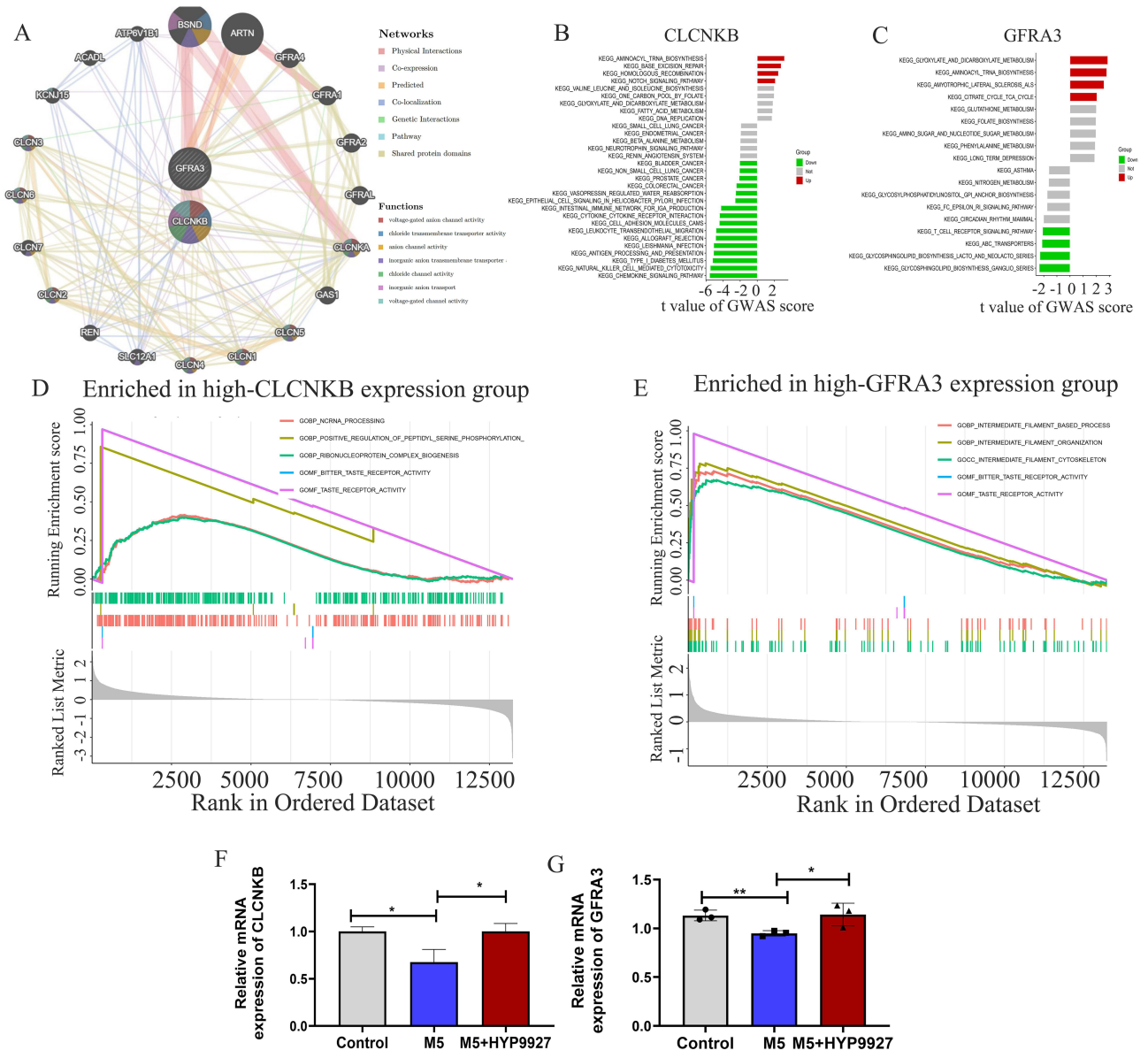

Figure 6 Functional Validation of CLCNKB and GFRA3 via Enrichment Analysis and Cellular Assays (**A**) Protein-protein interaction network of CLCNKB and GFRA3. (**B**) GSVA chart illustrating the enrichment of gene sets associated with CLCNKB. (**C**) GSVA chart illustrating the enrichment of gene sets associated with GFRA3. (**D**) GSEA chart illustrating the enrichment of gene sets associated with CLCNKB. (**E**) GSEA chart illustrating the enrichment of gene sets associated with GFRA3. (**F**) Changes in mRNA levels of CLCNKB in HaCaT cells after treatment with different factors; (**G**) Changes in mRNA levels of GFRA3 in HaCaT cells after treatment with different factors. *$p<0.05$, **$p<0.01$.

with gamma delta T cell infiltration; *GJA3* expression was positively correlated with M0 macrophage and follicular helper T cell infiltration; and *GJA3* expression was negatively correlated with resting mast cell infiltration (Figure 8A–F).

Mendelian Randomization Analysis of CLCNKB, GFRA3 and Cytokines

Causal relationships between *CLCNKB, GFRA3*, and various cytokines were further analyzed using the IVW method implemented in the TwoSampleMR package. As shown in Table 2, *CLCNKB* exhibited causal associations with IL-13, IL-10, IL-12, and TNFα, while *GFRA3* showed causal associations with IL-13, IL-12, and TGFβ. To facilitate visualization of the Mendelian Randomization (MR) analysis results, scatter plots were generated (Figure 9), displaying regression lines for IVW, MR-Egger, and weighted median analyses. Individual causal effect analysis revealed that increasing effects of individual single nucleotide polymorphisms (SNPs) on *GFRA3* corresponded to increased promoting effects on IL-12 and

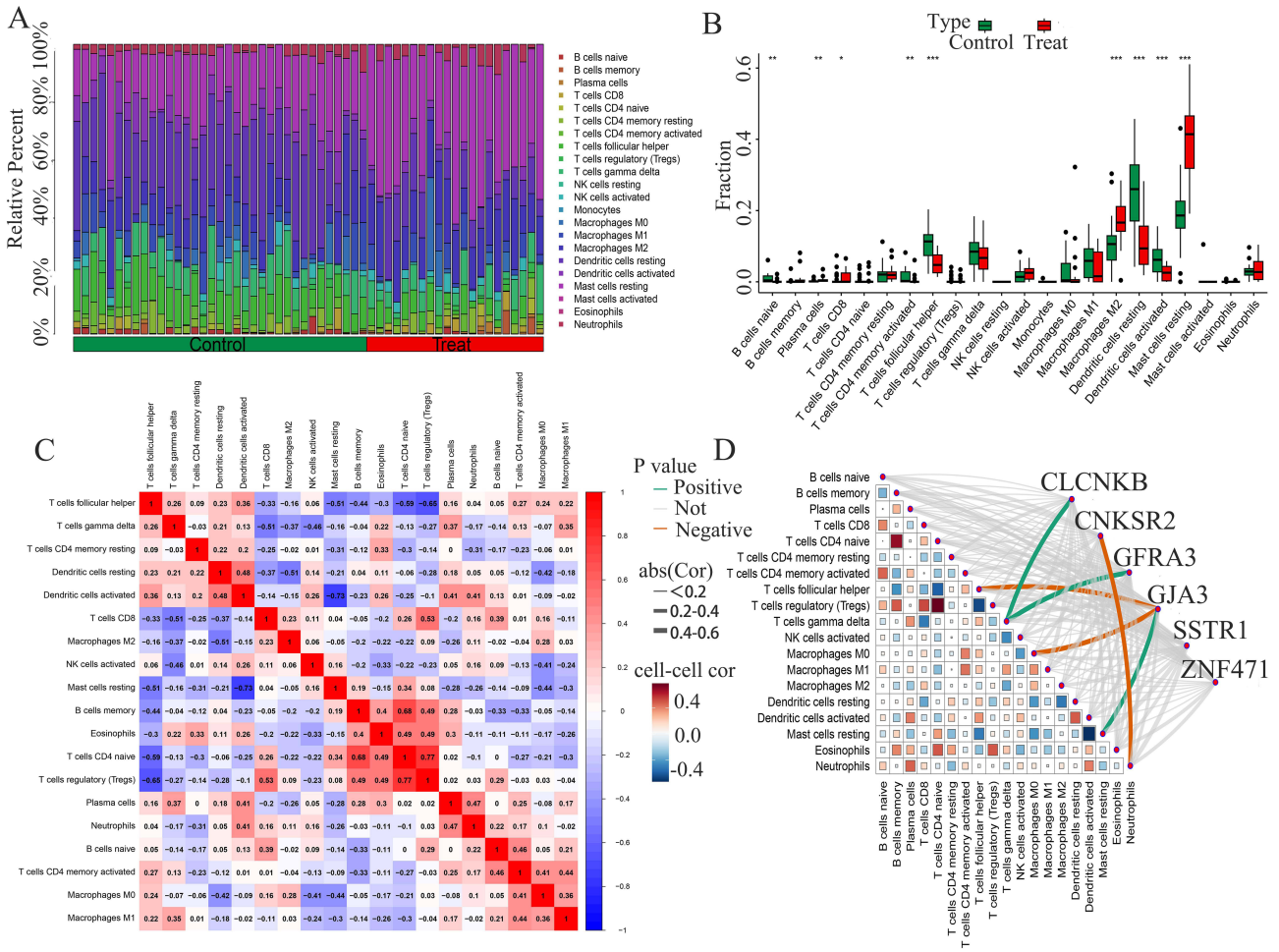

Figure 7 The immune cell infiltration landscape of psoriasis treated with IL17 inhibitors (**A**) The distribution ratio of 22 types of immune cells in the control group and treatment group patients. (**B**) Comparison of the distribution of 22 immune cell subtypes between the control group and the treatment group of psoriasis patients (green represents the control group, and red represents the treatment group). (**C**) Correlation matrix diagram of 22 immune cells. (**D**) Correlation between 6 differential genes and 22 immune cell subtypes (red indicates positive correlation, and green indicates negative correlation). * $p < 0.05$; ** $p < 0.01$; *** $p < 0.001$.

TGFβ and an increased inhibitory effect on IL-13 (Figure 9A–C). Similarly, increasing effects of individual SNPs on *CLCNKB* corresponded to increased inhibitory effects on IL-10, IL-12, IL-13, and TNFα (Figure 9D–G). The Cochran's Q test indicated no significant heterogeneity among the instrumental variables ($P > 0.05$), suggesting homogeneity at the genetic variant level. The MR-Egger intercept test, used to assess the presence of horizontal pleiotropy, showed intercept values close to zero with $P > 0.05$, indicating no significant pleiotropy. MR-PRESSO was employed to identify and correct for outliers, and the global test detected no significant outliers. Finally, after applying Bonferroni correction to the cytokine analyses, the results remained unchanged. These analyses collectively further validate the robustness of our findings.

Discussion

Studies have demonstrated that the IL-23/IL-17 inflammatory pathway plays a critical role in the development and progression of psoriasis.[26] Consequently, targeting the IL-17A signaling pathway is considered an effective therapeutic strategy for psoriasis. Numerous clinical studies have demonstrated the rapid and sustained efficacy of IL-17A inhibitors in improving psoriatic lesions, with favorable safety profiles.[27] Although significant progress has been made in elucidating the mechanism of action of IL-17A inhibitors in the treatment of psoriasis, the precise molecular mechanism remains unclear; more importantly, the mechanism of resistance to IL-17A inhibitors also needs further exploration.

In the present study, 113 machine learning algorithms were applied to select hub genes differentiating control and treatment groups, and a predictive model was constructed. Through rigorous evaluation and validation of multiple

https://doi.org/10.2147/CCID.S557553

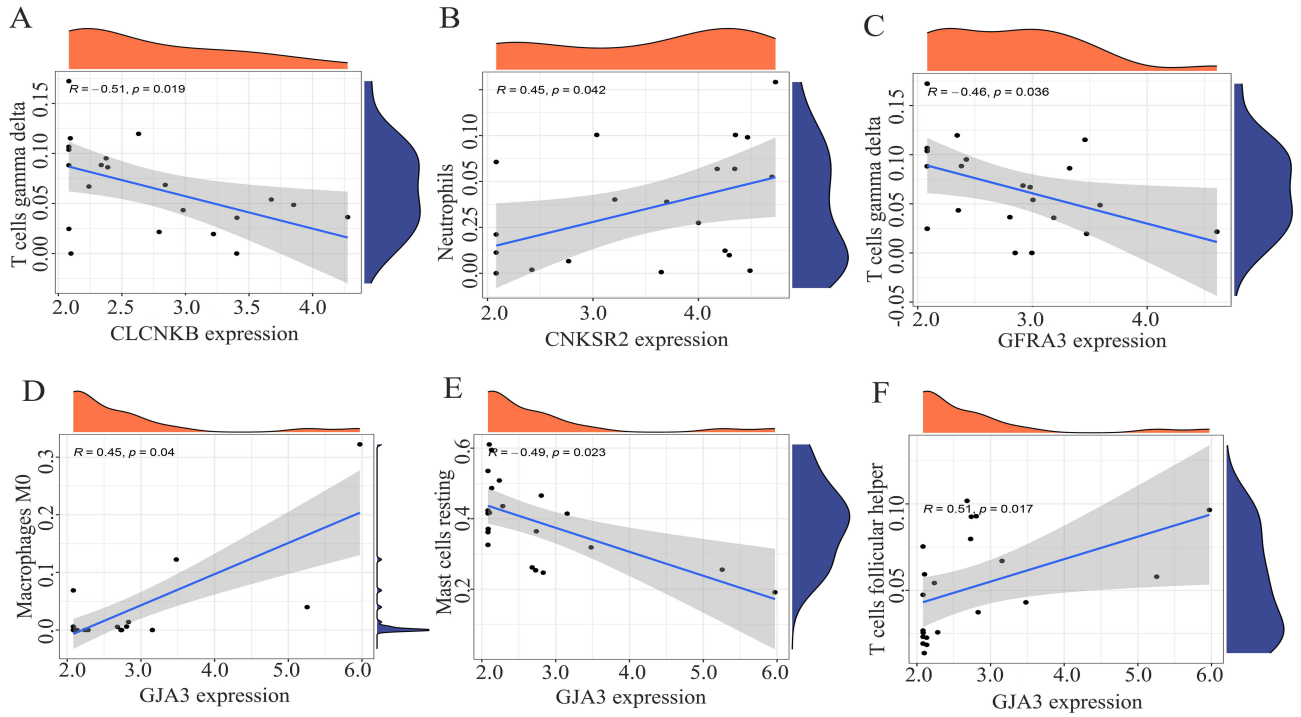

Figure 8 The correlation between CLCNKB, CNKSR2 and immune cell infiltration (**A**) The correlation between CLCNKB expression level and gamma delta T cells. (**B**) The correlation between CNKSR2 expression level and Neutrophils. (**C**) The correlation between GFRA3 expression level and gamma delta T cells. (**D**) The correlation between GJA3 expression level and M0 Macrophages. (**E**) The correlation between GJA3 expression level and resting Mast cells. (**F**) The correlation between GJA3 expression level and follicular helper T cells. The Orange area in the figure is the visualization of the Confidence Interval. The blue area is the visualization of the Regression Line.

models, the optimal model was selected. Comparison of the treatment and control groups revealed upregulation of *CLCNKB, GFRA3, ZNF471, CNKSR2*, and *SSTR1*, and downregulation of *GJA3* in the treatment group. Correlation analysis demonstrated significant relationships among these genes. Notably, *CLCNKB, GFRA3, SSTR1, ZNF471*, and *CNKSR2* exhibited high AUC values, suggesting their potential as accurate biomarkers for distinguishing between psoriasis control and treatment groups. These findings suggest that these genes and their associated pathways may play crucial roles in the efficacy of IL-17A inhibitors in psoriasis treatment. In vitro experiments further demonstrated that combined treatment with M5 and the IL-17 inhibitor HYP9927 significantly increased the expression of *CLCNKB* and *GFRA3*, suggesting that IL-17A upregulate the expression of these genes. Functional enrichment analysis indicated that *CLCNKB* is primarily involved in pathways such as chemokine signaling, natural killer cell-mediated cytotoxicity, antigen processing and presentation, leukocyte transendothelial migration, cytokine-cytokine receptor interaction, base excision repair, and homologous recombination. *GFRA3* is primarily associated with T cell receptor signaling and the tricarboxylic acid (TCA) cycle.

Table 2 Mendelian Randomization Analysis of GFRA3, CLCNK and Cytokines

Exposures	Outcomes	Methods	Number of SNPs	Beta	SE	MR *P*-val
CLCNKB	IL-13	IVW	18	−0.343	0.056	6.95e-10**
	IL-10	IVW	18	−0.296	0.056	1.53e-7**
	IL-12	IVW	18	−0.176	0.056	0.002**
	TNF-α	IVW	18	−0.291	0.056	2.53e-7**
GFRA3	IL-13	IVW	15	−0.234	0.114	0.041*
	IL-12	IVW	15	0.299	0.112	0.007**
	TGF-β	IVW	12	0.303	0.075	0.000**

Note: *p<0.05, **p<0.01.

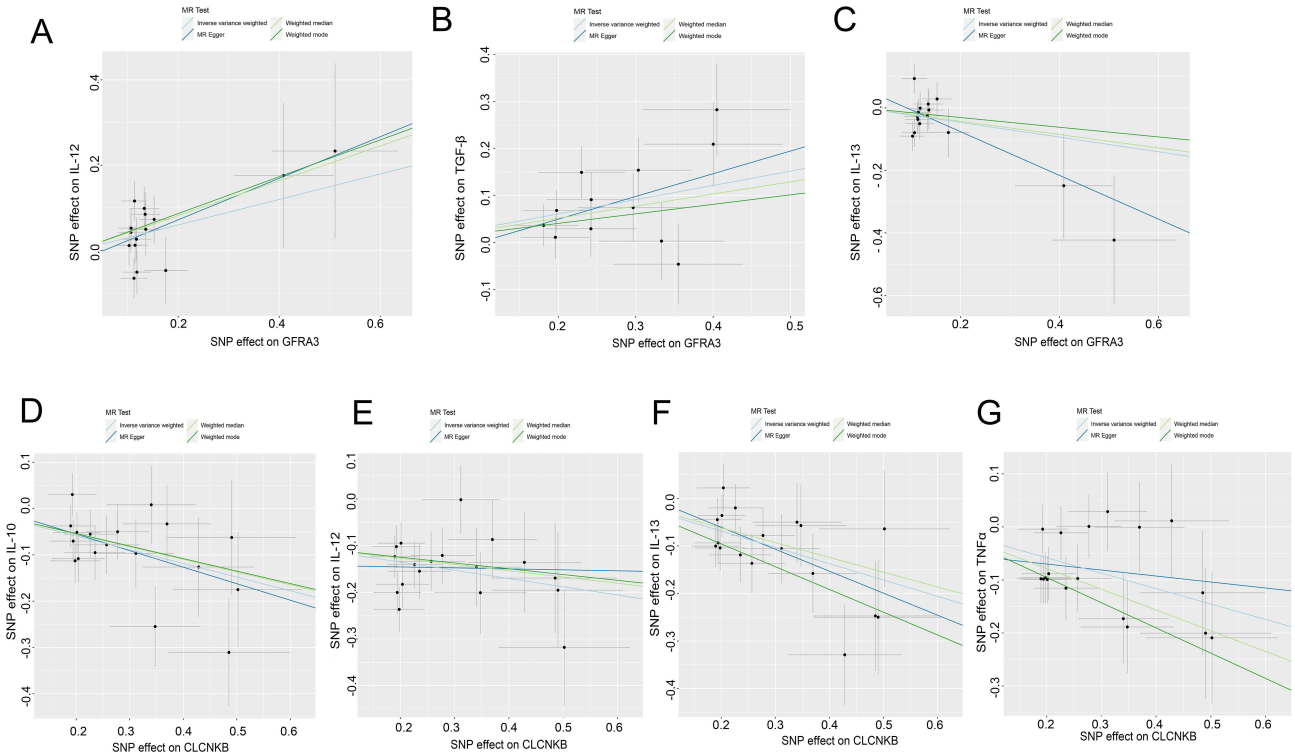

Figure 9 Scatter plot of causal effects of GFRA3, CLCNKB and cytokines in Mendelian randomization analysis (**A**) Scatter plot of causal effects between GFRA3 and IL-12. (**B**) Scatter plot of causal effects between GFRA3 and TGF-β. (**C**) Scatter plot of causal effects between GFRA3 and IL-13. (**D**) Scatter plot of causal effects between CLCNKB and IL-10. (**E**) Scatter plot of causal effects between CLCNKB and IL-12. (**F**) Scatter plot of causal effects between CLCNKB and IL-13. (**G**) Scatter plot of causal effects between CLCNKB and TNFα.

Psoriasis is a T-cell-mediated inflammatory disease, where abnormal infiltration and increased activity of specific T-cell subsets, such as γδ and βδ T cells, play a critical role in its pathogenesis.[28] The expression of *CLCNKB, CNKSR2, GFRA3*, and *GJA3* was significantly associated with immune cell infiltration patterns. Specifically, *CLCNKB* expression exhibited a negative correlation with γδ T cell infiltration, while *GFRA3* expression showed a negative correlation with βδ T cell infiltration. These findings suggest that *CLCNKB* and *GFRA3* may play a role in regulating the function and infiltration of these T cell subsets. Further Mendelian randomization analysis revealed causal associations between *CLCNKB, GFRA3*, and several cytokines. *CLCNKB* was associated with IL-10, IL-12, IL-13, and TNF-α, while *GFRA3* exhibited associations with IL-12, IL-13, and TGF-β. Cytokines such as IL-13, IL-10, IL-12, TNF-α, and TGF-β play significant roles in psoriasis[29] IL-10, a key anti-inflammatory cytokine primarily secreted by regulatory T cells (Tregs), B cells, and macrophages, suppresses Th1 and Th17 inflammatory responses and is significantly reduced in patients with psoriasis[29,30] IL-12 promotes Th1-mediated immune responses and is critically involved in the development of psoriasis.[31] TNF-α, a canonical pro-inflammatory cytokine, activates the NF-κB pathway, promoting keratinocyte hyperproliferation and immune cell recruitment.[32] TGF-β, while exhibiting anti-inflammatory properties under normal conditions, can promote Th17 differentiation under pathological conditions, thereby exacerbating psoriatic inflammation.[33] Therefore, IL-17A, as the central effector cytokine in psoriasis, may interact with multiple other cytokines, including IL-13, IL-10, IL-12, TNF-α, and TGF-β, through various immune pathways. These interactions collectively influence the development and severity of psoriasis, forming a complex network of effects. Our findings suggest that IL-17A inhibitors may indirectly modulate psoriasis progression by targeting *CLCNKB* and *GFRA3* as key immunoregulatory factors.

This study reveals a novel mechanism of IL-17A inhibitors in psoriasis treatment, involving the modulation of CLCNKB and GFRA3 pathways beyond direct IL-17A pathway inhibition. Mutations or dysregulation of these genes may influence drug efficacy and contribute to immune escape, suggesting their potential as combination therapy targets. The key differences between this study and previous multi-cohort WGCNA/ML analyses lie in two aspects: at the data

level, it specifically focuses on psoriasis patients before and after IL-17A inhibitor treatment in the GEO database, resulting in a significantly distinct sample composition compared to prior studies; at the methodological level, it innovatively introduced MR analysis to achieve multi-dimensional validation, while strictly satisfying the key assumptions of MR analysis to demonstrate robust causal associations. This study has limitations that should be acknowledged, including the relatively small sample size and the absence of clinical efficacy data correlated with observed genomic changes. Further investigation of the functions and regulatory mechanisms of the identified differentially expressed genes in cellular and animal models is warranted. While IL-17A inhibitors have significantly advanced psoriasis treatment, their mechanisms of action remain complex, involving multiple pathways and immune cell subsets. A comprehensive understanding of these changes will facilitate the discovery of novel therapeutic targets and strategies, ultimately guiding the precise application of IL-17A inhibitors to optimize outcomes for psoriasis patients.

Conclusion

This study provides novel insights into the mechanisms of IL-17 inhibitor response in psoriasis, revealing that upregulation of CLCNKB and GFRA3, along with cytokine dysregulation (eg, IL-13, IL-10, IL-12, TGF-β, TNF-α), may contribute to on-treatment biological changes consistent with resistance/relapse hypotheses. While these findings offer a promising approach for predicting clinical outcomes, their clinical utility requires further validation through patient-level response phenotyping and longitudinal studies in real-world settings to further facilitate the clinical translation of novel psoriasis treatment strategies targeting CLCNKB and GFRA3.

Funding

The Natural Science Basic Research Program of Shaanxi Province (2024JC-YBJN-0783) and the National Natural Science Foundation of China (No. 8197293) supported this study.

Disclosure

The authors declared that no competing interest exists.

References

1. Wu JJ, Kavanaugh A, Lebwohl MG, et al. Psoriasis and metabolic syndrome: implications for the management and treatment of psoriasis. *J Eur Acad Dermatol Venereol*. 2022;36(6):797–806. doi:10.1111/jdv.18044
2. Weber B, Merola JF, Husni ME, et al. Psoriasis and cardiovascular disease: novel mechanisms and evolving therapeutics. *Curr Atheroscler Rep*. 2021;23(11):67. doi:10.1007/s11883-021-00963-y
3. Zhou S, Lei L, Jiang L, et al. Polycyclic aromatic hydrocarbons exposure associated with increased risk of psoriasis. *Exp Dermatol*. 2024;33(8):e15166. doi:10.1111/exd.15166
4. Fan W, Lei N, Zheng Y, et al. Oral microbiota diversity in moderate to severe plaque psoriasis, nail psoriasis and psoriatic arthritis. *Sci Rep*. 2024;14(1):18402. doi:10.1038/s41598-024-69132-w
5. Chen L, Chen H, Mo L, et al. Spatial distribution of residential environment, genetic susceptibility, and psoriasis: a prospective cohort study. *J Glob Health*. 2024;14:04139. doi:10.7189/jogh.14.04139
6. Von Meyenn L, Bertschi NL, Schlapbach C. Targeting T cell metabolism in inflammatory skin disease. *Front Immunol*. 2019;10:2285. doi:10.3389/fimmu.2019.02285
7. Cibrian D, Castillo-González R, Fernández-Gallego N, et al. Targeting L-type amino acid transporter 1 in innate and adaptive T cells efficiently controls skin inflammation. *J Allergy Clin Immunol*. 2020;145(1):199–214.e11. doi:10.1016/j.jaci.2019.09.025
8. Abboud E, Chrayteh D, Boussetta N, et al. Skin hepcidin initiates psoriasiform skin inflammation via Fe-driven hyperproliferation and neutrophil recruitment. *Nat Commun*. 2024;15(1):6718. doi:10.1038/s41467-024-50993-8
9. Yin L, Zhang E, Mao T, et al. Macrophage P2Y(6)R activation aggravates psoriatic inflammation through IL-27-mediated Th1 responses. *Acta Pharm Sin B*. 2024;14(10):4360–4377. doi:10.1016/j.apsb.2024.06.008
10. Sieminska I, Pieniawska M, Grzywa TM. The immunology of psoriasis-current concepts in pathogenesis. *Clin Rev Allergy Immunol*. 2024;66(2):164–191. doi:10.1007/s12016-024-08991-7
11. Sun X, Liu L, Wang J, et al. Targeting STING in dendritic cells alleviates psoriatic inflammation by suppressing IL-17A production. *Cell Mol Immunol*. 2024;21(7):738–751. doi:10.1038/s41423-024-01160-y
12. Feldman SR, Narbutt J, Girolomoni G, et al. A randomized, double-blind, Phase III study assessing clinical similarity of SB17 (proposed ustekinumab biosimilar) to reference ustekinumab in subjects with moderate-to-severe plaque psoriasis. *J Am Acad Dermatol*. 2024;91(3):440–447. doi:10.1016/j.jaad.2024.04.045
13. Veerasubramanian PK, Wynn TA, Quan J, et al. Targeting TNF/TNFR superfamilies in immune-mediated inflammatory diseases. *J Exp Med*. 2024;221(11). doi:10.1084/jem.20240806

14. Yatsuzuka K, Muto J, Shiraishi K, et al. Paradoxical eczema associated with interleukin-17A inhibitor use in a patient with generalized pustular psoriasis accompanied by asthma. *Cureus*. 2024;16(7):e64680. doi:10.7759/cureus.64680
15. Yousif J, Al-Dehneem R, Kaskas N, et al. A case series of patients with eczematous eruptions following IL-17 Inhibitor treatment for psoriasis vulgaris. *J Drugs Dermatol*. 2023;22(12):1225–1227. doi:10.36849/JDD.7388
16. Busard CI, Cohen AD, Wolf P, et al. Biologics combined with conventional systemic agents or phototherapy for the treatment of psoriasis: real-life data from PSONET registries. *J Eur Acad Dermatol Venereol*. 2018;32(2):245–253. doi:10.1111/jdv.14583
17. de la Brassinne M, Ghislain PD, Lambert JL, et al. Recommendations for managing a suboptimal response to biologics for moderate-to-severe psoriasis: a Belgian perspective. *J DermatolTreat*. 2016;27(2):128–133. doi:10.3109/09546634.2015.1086476
18. Langfelder P, Horvath S. WGCNA: an R package for weighted correlation network analysis. *BMC Bioinf*. 2008;9:559. doi:10.1186/1471-2105-9-559
19. Moon I, LoPiccolo J, Baca SC, et al. Machine learning for genetics-based classification and treatment response prediction in cancer of unknown primary. *Nat Med*. 2023;29(8):2057–2067. doi:10.1038/s41591-023-02482-6
20. Newman AM, Liu CL, Green MR, et al. Robust enumeration of cell subsets from tissue expression profiles. *Nat Methods*. 2015;12(5):453–457. doi:10.1038/nmeth.3337
21. Ou HB, Wei Y, Liu Y, et al. Characterization of the immune cell infiltration landscape in lung adenocarcinoma. *Arch Biochem Biophys*. 2022;721:109168. doi:10.1016/j.abb.2022.109168
22. Burgess S, Butterworth A, Thompson SG. Mendelian randomization analysis with multiple genetic variants using summarized data. *Genet Epidemiol*. 2013;37(7):658–665. doi:10.1002/gepi.21758
23. Burgess S, Thompson SG. Interpreting findings from Mendelian randomization using the MR-Egger method. *Eur J Epidemiol*. 2017;32 (5):377–389. doi:10.1007/s10654-017-0255-x
24. Zhang M, Zeng Q, Zhou S, et al. Mendelian randomization study on causal association of IL-6 signaling with pulmonary arterial hypertension. *Clin Exp Hypertens*. 2023;45(1):2183963. doi:10.1080/10641963.2023.2183963
25. Liu M, Zhang G, Wang Z, et al. FOXE1 contributes to the development of psoriasis by regulating WNT5A. *J Invest Dermatol*. 2023;143(12):2366–77.e7. doi:10.1016/j.jid.2023.04.035
26. Ghoreschi K, Balato A, Enerbäck C, et al. Therapeutics targeting the IL-23 and IL-17 pathway in psoriasis. *Lancet*. 2021;397(10275):754–766. doi:10.1016/S0140-6736(21)00184-7
27. Adams R, Maroof A, Baker T, et al. Bimekizumab, a novel humanized igg1 antibody that neutralizes both IL-17A and IL-17F. *Front Immunol*. 2020;11:1894. doi:10.3389/fimmu.2020.01894
28. Sivasami P, Elkins C, Diaz-Saldana PP, et al. Obesity-induced dysregulation of skin-resident PPARγ(+) Treg cells promotes IL-17A-mediated psoriatic inflammation. *Immunity*. 2023;56(8):1844–61.e6. doi:10.1016/j.immuni.2023.06.021
29. Kutwin M, Migdalska-Sęk M, Brzeziańska-Lasota E, et al. An analysis of IL-10, IL-17A, IL-17RA, IL-23A and IL-23R expression and their correlation with clinical course in patients with psoriasis. *J Clin Med*. 2021;10(24):5834. doi:10.3390/jcm10245834
30. Mollazadeh H, Cicero AFG, Blesso CN, et al. Immune modulation by curcumin: the role of interleukin-10. *Crit Rev Food Sci Nutr*. 2019;59 (1):89–101. doi:10.1080/10408398.2017.1358139
31. Zhou J, Shen JY, Liu LF, et al. Indirect regulation and equilibrium of p35 and p40 subunits of interleukin (IL)-12/23 by ustekinumab in psoriasis treatment. *Med Sci Monit*. 2020;26:e920371.
32. Qiu XN, Hong D, Shi ZR, et al. TNF-α promotes CXCL-1/8 production in keratinocytes by downregulating galectin-3 through NF-κB and hsa-miR -27a-3p pathway to contribute psoriasis development. *Immunopharmacol Immunotoxicol*. 2023;45(6):692–700. doi:10.1080/ 08923973.2023.2229510
33. Singh TP, Huettner B, Koefeler H, et al. Platelet-activating factor blockade inhibits the T-helper type 17 cell pathway and suppresses psoriasis-like skin disease in K5.hTGF-β1 transgenic mice. *Am J Pathol*. 2011;178(2):699–708. doi:10.1016/j.ajpath.2010.10.008